JOURNAL OF OPTOELECTRONICS AND ADVANCED MATERIALS Vol. 8, No. 6, December 2006, p. 2051 - 2057

Quadrupole and chemical shift interactions in crystalline and amorphous chalcogenides

D. C. BOBELA, P. CRAIG TAYLOR[a*]
Department of Physics, University of Utah Salt Lake City, Utah
[a]Department of Physics, Colorado School of Mines, Golden, Colorado

This paper reviews the general features of magnetic resonance spectra specific to the amorphous chalcogenide materials. We discuss the dominant interactions that influence the local bonding structure. We show how to parameterize the interactions and simulate their spectra in frequency space. In contrast to the crystalline phase, the amorphous material exhibits variations in the local bonding structure. We discuss how to account for these variations and compare the resulting frequency space spectra with their crystalline counterparts.

(Received October 10, 2006; accepted November 2, 2006)

Keywords: Chalcogenide glasses, Nuclear magnetic (and quadrupole) resonance, Chemical shift, Powder pattern

1. Introduction

Recent technological applications of some chalcogenide materials, compounds containing a group VI atom, have prompted studies of the local atomic structure of the amorphous phase. In the case of $Ge_2Sb_2Te_5$, metastability in the local bonding structure is responsible for its usefulness as a phase-change memory material [1, 2]. There is no consensus on the exact phase-change mechanism, which is partly due to the inadequacy of standard scattering techniques to probe the structure of the amorphous phase. Magnetic resonance methods are well suited to study local structural order. In this technique, structural information is encoded as an oscillating voltage caused by the nuclear spin.

Magnetic resonance methods are particularly fruitful when studying the Sb_2Te_3 – GeTe tie line, which includes $Ge_2Sb_2Te_5$. The ^{121}Sb and ^{125}Te nuclei have gyromagnetic ratios similar to ^{13}C and therefore can be studied on most commercially available magnetic resonance set-ups. In principle, local order can be studied as a function of the stoichiometry and phase of the material.

Magnetic resonance, methods have long been used to probe the local bonding structure of disordered materials (see for instance, refs. 3 and 4 and references therein). In solid-state magnetic resonance, the wealth of local structural information results from the functional forms of the total nuclear Hamiltonian. Interactions have an inherent spatial dependence and these dependences sometimes give rise to the unusual spectra in frequency space. In general, the frequency spectrum for each interaction can be calculated and used as a fingerprint when interpreting the experimental data. In the easiest case, there is a dominant interaction and the resulting spectrum can be explained in terms of the parameters that describe the interaction provided that the spectral features are well resolved. When the various interaction strengths are comparable, the spectrum consists of a superposition of each fingerprint, and the interpretation must include all relevant parameters.

In the remainder of the paper, we describe the magnetic resonance data typically observed in crystalline and amorphous chalcogenides. We will discuss the role of disorder and the interactions specific to these systems. We demonstrate the consequences of varying the parameters with spectral simulations, for which we present a general calculation scheme.

2. Amorphous materials and magnetic resonance spectra

In general, magnetic resonance methods valid for crystalline lattices also apply to amorphous systems. This fact results primarily from the invariance of chemical bond lengths. Nearest neighbor distances are generally preserved in the amorphous phase [5]. Therefore, the magnitude of the nearest neighbor interactions, such as the inter-nuclear dipole-dipole coupling, will be approximately invariant. Bond angles are less well defined, and this degree of freedom allows for distortions from those that occur in the crystal lattice. These distortions affect interactions that have dependences on the direction of the applied magnetic field with respect to the interaction's principle components, such as the chemical shift and quadrupole interactions.

What causes the major differences between the spectra in the crystalline and amorphous phases? The answer should depend on the degree of disorder occurring in the local structural order. In crystalline lattices, those exhibiting long-range order, there exists a well-defined set of translation vectors to go from site to site. There is an inescapable amount of disorder, due to thermodynamics, but in a "good" crystal, it is insufficient to affect the bulk properties of the material [5]. The crystalline lattice is also "rigid" in the sense that bonding requirements for each atom are satisfied by an underlying periodic lattice. Once this rigidity is relaxed, the lattice can accommodate

structural changes manifested as strained bonds and bond angle variations. The lattice begins to loose its long-range order, but short-range (nearest-neighbor) structure similar to the crystalline phase still exists. This property is vital to a good glass former, such as the chalcogen compounds. However, more rigid systems, such as a-Si:H, exhibit similar features. A simplified picture of the amorphous phase might consist of a collection of randomly oriented sites that have nearest neighbor configurations similar to the crystalline phase. Such a system would exhibit similar resonance spectra, since each local unit has the same structure. However, introducing strained bonds and varying bond angles will produce departures from the unique building blocks. Then, the local structured unit is preserved, only on average and this distribution of local environments produces a distribution of interactions. Consequently, the resonance spectrum in the glassy system becomes a superposition of spectra that reflects the distribution in structural parameters.

Mathematically, the superposition idea has a simple representation. In general terms, the superposition of a function describing the resonance intensity that depends on frequency, *S(ν)*, (intensity could refer to absorption, induced voltage etc.) can be written:

$$S(\nu) \propto \sum_{s_i} S(\nu_i; s_i) P(\nu_i; s_i), \qquad (1)$$

where $S(\nu_i; s_i)$ is understood to be the frequency response for a particular set of parameters, s_i. The function $P(\nu_i; s_i)$ represents a distribution function accounting for the variations in the parameters. $P(\nu_i; s_i)$ is commonly assumed to be a Gaussian function characterized by the average, s_{ave}, and full width at half maximum, σ_{FWHM} [3] . For crystalline systems, $P(\nu_i; s_i)$ will approach a delta function to reflect the well-defined local unit. When approaching the glassy phase, σ_{FWHM} increases as the lattice accommodates larger structural distortions. One immediate consequence of a non-zero σ_{FWHM} , is that the overlapping spectra tend to smear features that could be used to deduce structural parameters. This effect is demonstrated in Fig. 1, which contrasts the calculated nuclear magnetic resonance (NMR) spectrum in frequency space for a single and a distribution of quadrupole coupling constants. Details of how to generate $S(\nu)$ will be discussed in a later section. For the present discussion, the parameters have been choosen to represent a typical NMR data set resulting from a "weak" quadrupole interaction. The operating frequency, set by the magnetic field strength, has been suppressed so that spectral center occurs at 0 MHz. For a single set of parameters, s_o, the spectrum contains well-defined features as shown in Fig. 1a. The spectrum in Fig. 1b results when the coupling constants are distributed about s_o. Here we have assumed $P(\nu_i; s_i)$ to be a Gaussian distribution with $s_{ave} = s_o$ and $\sigma_{FWHM} = 30\%\ s_o$.

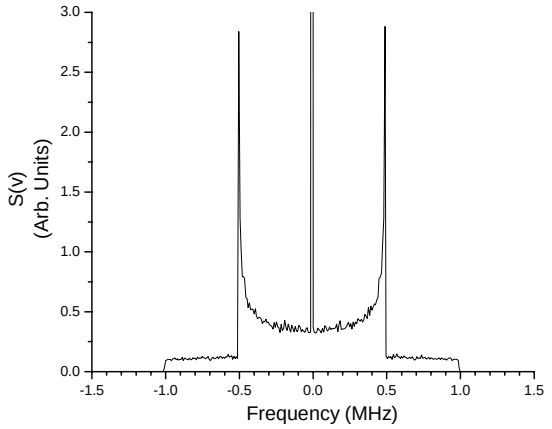

a

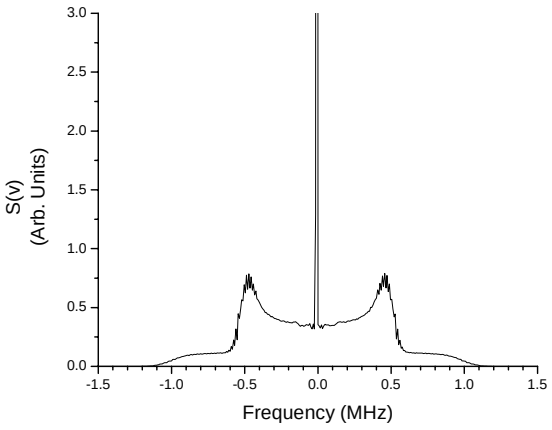

b

Fig. 1. Frequency space NMR spectra for nuclear spin = 3/2. For both plots, ν_L = 100 MHz. See text for parameter definitions. a) Simulation with ν_q = 0.166% of ν_L , η = 0. b) Simulation for a distribution of ν_q with $s_{ave} = \nu_q$, σ_{FWHM} = 30% of ν_q , η = 0.

Increasing σ_{FWHM} essentially amounts to a loss of information. While the divergences at ± 0.5 MHz seem adequately resolved, the shoulders at ± 1.0 MHz have been smoothed. In experimental spectra, both features may be difficult to measure accurately if the signal is small.

Parameter distributions are also observed in the pure nuclear quadrupole resonance (NQR) experiment. Fig. 2 shows NQR data for the As_2Se_3 glass [6]. A Gaussian distribution of quadrupole coupling constants with s_{ave}= 57.9 MHz, σ_{FWHM} = 2.9 MHz is needed to describe data. In the crystalline phase, there are two inequivalent arsenic sites giving rise to two NQR frequencies [7]. These transitions at 56.07 and 60.25 MHz are also depicted in Fig. 2.

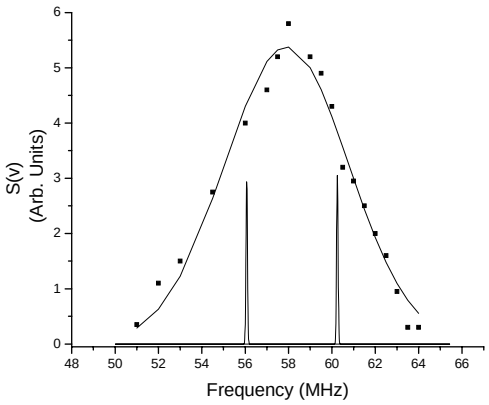

Fig. 2. Solid Circles represent NQR experimental spectra in frequency space for amorphous As_2Se_3. The data are fit with a Gaussian distribution of ν_q with s_{ave} = 57.9 MHz, σ_{FWHM} = 2.86 MHz. For reference, the NQR frequencies of the two arsenic sites occurring in crystalline As_2Se_3 are shown below the experimental data.

3. Spectral simulations

Magnetic resonance simulations start with the Hamiltonian for the nuclear spin system, which determines the frequency spectrum, or, in the time domain, the time evolution of the spin states. The calculation consists of solving the eigenvalue problem with a particular Hamiltonian matrix and basis set. Once the eigen-energies are known, various manipulations of the Hamiltonian, determined by the pulse sequence used in the magnetic resonance experiment, can be used to probe the transitions between eigen-energies. Reference 8 provides the mathematical formalism used for making such computations. Many excellent computational programs also exist in the NMR literature [9-13]. Those listed in refs. 9-13 are designed to allow the user great flexibility in designing and simulating magnetic resonance experiments.

The simulation procedure outlined here represents the most basic, brute force approach to spectral simulation. In the chalcogenide glasses, there will be a Zeeman H_L, a quadrupole, H_q, and chemical shift, H_{CS}, interaction. Therefore the total Hamiltonian is written as:

$$H_T = H_q + H_{CS}(\theta,\phi,\varphi) + H_L(\theta,\phi,\varphi), \qquad (2)$$

where θ, ϕ, and φ represent the Euler angles with respect to the H_q coordinate system. The forms for H_q and H_{CS} + H_L are given in eqs. 5 and 7, respectively. In the pure NQR experiment, the magnetic field terms of eq. 2 are set equal to 0. In general, the set of principle axes for H_q does not correspond with the laboratory coordinate system. But because the H_{CS} and H_L have simpler operator forms, we have chosen to write H_{CS} and H_L in terms of the H_q coordinate system.

For the working basis of spin states, we choose the set of states labeled by the z-component (m_z) of spin angular momentum. Then, an orientation $\{\theta, \phi, \varphi\}$ and set of Hamiltonian parameters is chosen. The Hamiltonian is diagonalized to give the eigenstates and corresponding eigen-energies. For both NQR and NMR, the transitions are probed using a single radio frequency pulse oriented in the x-direction of the laboratory frame, H_p. The transition intensity is therefore related to the transition probability:

$$Intensity \propto \left|\left\langle f \left| H_p(\theta,\phi,\varphi) \right| i \right\rangle\right|^2, \qquad (3)$$

where $\left|i\right\rangle$ and $\left\langle f\right|$ represent the initial and final spin states of the diagonalized system.

Many of the chalcogenide materials are not available as single crystals. It is therefore necessary to study the material in powdered form, which can fit easily into test tubes and sample chambers. Crystallites in the powder can have any $\{\theta, \phi, \varphi\}$, and the transitions for each set must be computed. The resulting array of transition frequencies and intensities constitutes the "powder pattern". For a discussion of various methods of powder averaging, the reader is referred to ref. 14. The most basic powder averaging scheme is to generate a large, random set of $\{\theta, \phi, \varphi\}$ and compute the weighted transitions (to account for the probability of selecting that particular orientation) for each resulting Hamiltonian. This method neglects any of the Hamiltonian symmetries that may facilitate faster computations [14].

4. Interactions and sample spectra

There are several detailed treatments of the spectra resulting from the quadrupole and chemical shift Hamiltonians [3, 15-17]. In the present work, we present a brief overview of the quadrupole and chemical shift Hamiltonians and how they influence the interpretation of magnetic resonance spectra. An understanding of these basic interactions is discussed with an emphasis on the chalcogenide glasses. We demonstrate the relationship between the Hamiltonian parameters and the measured frequency spectra for a few simple cases.

a.) *The Quadrupole Interaction*

Chalcogenide compounds usually contain atoms whose nuclear spin, I, is greater than ½ (As_2S_3, Sb_2Te_3, etc.) Nuclei satisfying this condition have non-spherical nuclear charge, and these departures from spherical symmetry produce a nuclear quadrupole moment, (eQ). This quantity will couple to any electric field gradient imposed by the surrounding electronic cloud. In general, the electric field gradient, is defined by a 3x3 tensor that represents the spatial variation in the electrostatic potential at the nucleus. When the field gradient is only due to charges external to the nucleus, the tensor is symmetric

and traceless, which reduces the number of independent parameters from nine to five [18]. It is then customary to represent the tensor in a set of principal axes. In this form the tensor has two independent components. The resulting interaction, which is a tensor-scalar product between the electric field gradient and *eQ*, has two adjustable parameters, the quadrupole coupling constant, ν_q, and the asymmetry parameter, η. The former is a measure of the interaction strength, while the latter is a measure of the departure of the electric field gradient from axial symmetry:

$$\nu_q = \frac{(eQ)eV_{zz}}{h}\frac{1}{4I(2I-1)}; \qquad (4a)$$

$$\eta = \frac{\left|V_{xx} - V_{yy}\right|}{\left|V_{zz}\right|} \text{ where } \left|V_{zz}\right| > \left|V_{yy}\right| > \left|V_{xx}\right|, \qquad (4b)$$

where *h* is Planck's constant, e is the charge of an electron, $V_{ii} = \partial^2 V / \partial x_i \partial x_i$ are the non vanishing electric field gradient components, and ν_q is expressed in Hertz. Because $V_{xx} + V_{yy} + V_{zz} = 0$, in equation 4b, $0 \le \eta \le 1$, where η = 0 represents the axially symmetric case. Perfectly cubic and perfectly tetrahedrally coordinated nuclear sites are examples where the bonding symmetry produces a vanishing electric field gradient. The full quadrupole Hamiltonian (in Hertz) used in spectral simulations can be expressed as [18]:

$$H_q = \nu_q[(3I_z^2 - I^2) + \eta(I_x^2 - I_y^2)], \qquad (5)$$

where I_i are the dimensionless spin operators. Diagonalization of eq. 5 is trivial in the case of axial symmetry; the eigenstates are the set of m_z spin states. Since the operator I_z^2 is degenerate in m_z, the pure NQR experiment contains *I – 1/2* transitions for half-integer nuclei, irrespective of orientation. When $\eta \neq 0$, the degeneracy is lifted since the eigenstates become mixtures of the m_z basis set. Therefore the measured resonance shifts in frequency. These qualitative features are shown in Fig. 3, which represents the pure NQR experiment for the axially symmetric and η = 1, *I = 3/2* systems. The spectrum is computed with ν_q = 10.04 MHz, which is representative of the coupling constant in crystalline As_2Se_3. The otherwise delta functions at ~ 60 MHz and ~ 69.5 MHz have been broadened to ~ 100 kHz FWHM, which is typically measured in crystalline chalcogenides. Usually, in the pure NQR experiment, the dipolar interactions are much smaller than the measured line width. Therefore it is the distributions of ν_q and η, that produce a superposition of transitions, which account for the majority of the spectral breadth.

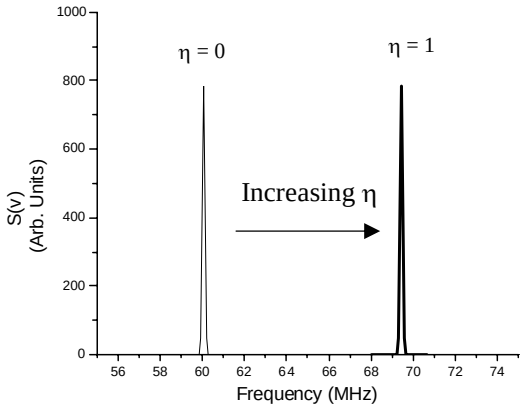

Fig. 3. Pure NQR spectra in frequency space for the I = 3/2 system with ν_q = 10.04 MHz. The resonance near 60 MHz corresponds to the axially symmetric, η = 0 case. Increasing η shifts the resonance to higher frequency until at ~ 68 MHz, η = 1.

The high field, $\nu_L >> \nu_q$, NMR experiment for an *I = 3/2* system with η = 0 is demonstrated in Fig. 1a. We have chosen ν_L = 100 MHz and ν_q = 0.166 % of ν_L. The central transition is essentially a delta function at ν_L and therefore it extends off scale. For intermediate values of η, the divergences shift inward, towards ν_L until η = 1, whereby the divergences collapse into a single transition at ν_L, but the shoulders remain at $\pm 6\nu_q$. As long as the high field limit applies, the positions of divergences and shoulders are independent of ν_L [3].

At lower fields, the magnetic resonance spectra become increasingly complicated. Diagonalization of the total Hamiltonian, $H_L + H_q$, produces non-intuitive mixtures of the m_z basis states. The frequency spectra sometimes broaden to include additional transitions that were forbidden in the high field limit. In the chalcogen glasses, ν_q is typically large enough compared to commercially available magnetic fields such that higher order effects contribute to the spectra. In most cases, the spectra are broader than the detection bandwidth. In severely broadened spectra, the intensity at any point may fall below the detection limit thus rendering the measurement impossible. The standard "low field" NMR experiment for the ^{75}As system, with ν_q = 10.04 MHz and η = 0 would be extremely difficult, even if the largest static magnetic fields (~20 Tesla) are used.

In addition to the loss of signal due to the large spectral breadth, sweeping the frequency over such a range requires impractically large modifications to the transmission and detection schemes. A more practical method is to sweep the magnetic field while keeping the excitation frequency constant. This technique has been used to study local arsenic bonding sites in As_xS_{1-x} and As_xSe_{1-x} glasses [6].

When the high field limit breaks down, the central transition is broadened. In the 2nd order perturbation limit, the divergence and shoulder positions of the central transition have analytical solutions which depend on ν_L

[3]. The general features are demonstrated in Fig. 4, which shows a $I = 3/2$ powder pattern for $\nu_L = 100$ MHz, $\nu_q = 2\%$ of ν_L. When compared to Fig. 1a, we see that shoulders now cover ± 6 MHz. The central transition has broadened into a set of divergences, which are not symmetrically centered about the origin.

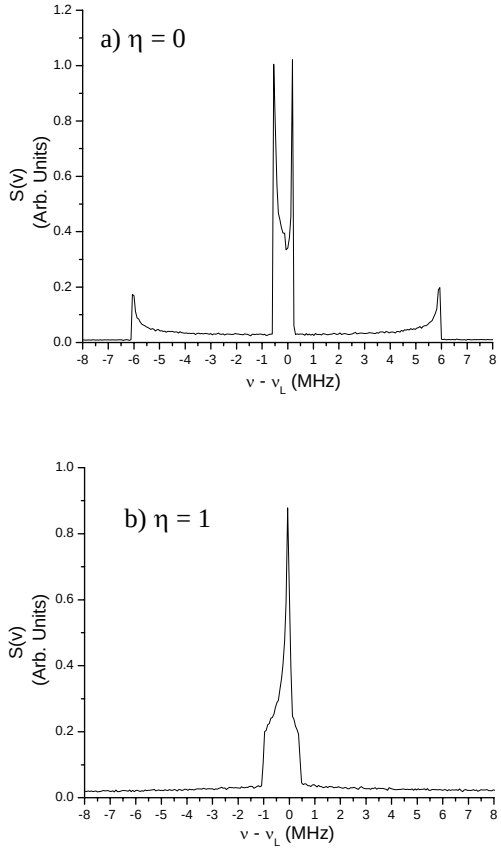

Fig. 4. Low field NMR frequency spectra for the I = 3/2 system where ν_L = 100 MHz and ν_q = 2% of ν_L. The spectra have been runcated at ±8 MHz. a) $\eta = 0$, b) $\eta = 1$.

b.) Magnetic shift interactions

Changes in nuclear resonance due to electronic effects have been well known and studied since the 1950's [19]. In semiconductors, where the conductivities are small, the so-called chemical shift results from magnetically induced electronic currents in the core states. The currents produce their own magnetic fields at the nuclear site that compete with the applied field. Since the effect increases for states with increasing angular momentum, heavier nuclei experience greater chemical shifts.

The same tensor mathematics used in the quadrupole case can describe the chemical shift. The tensor does not, in general, display the same symmetries as that of the quadrupole interaction. When transformed to a set of principle axes, the tensor can be written as the sum of a diagonal and off-diagonal matrix [8]. Three adjustable parameters are needed to completely specify the interaction. The diagonal matrix requires one parameter, which is a measure of the overall isotropic shift in magnetic field. For the quadruple case, this parameter is 0 due to the requirement that the tensor be traceless. The off diagonal matrix requires two parameters: one for scaling the interaction strength and one specifying the degree of asymmetry.

The chemical shift can be thought of as an arbitrarily oriented applied field:

$$H_{CS} = \nu_L[\sigma_z I_z + \sigma_x I_x + \sigma_y I_y], \qquad (6)$$

where σ_i is a dimensionless number that represents the field contribution along the i^{th} direction. Assuming the applied field is along the z-direction, the total applied field Hamiltonian can be written as [3]:

$$H_{TL} = H_L + H_{Cs} = \nu_L[(1-\sigma_z)I_z - \sigma_x I_x - \sigma_y I_y]. \qquad (7)$$

The chemical shift does not influence the NQR spectra, but it will introduce its own powder pattern in the NMR experiment. If no other interactions are present, the chemical shift powder patterns will have the form shown in Fig 5. Values of σ_i, determine the positions of shoulders and divergences as indicated in the plot. Perhaps one of most easily identifiable effects is the overall shift in the spectral center of gravity. This so-called isotropic shift is given by [8]:

$$\nu_{iso} = \nu_L \frac{\left|\sigma_z + \sigma_x + \sigma_y\right|}{3}. \qquad (8)$$

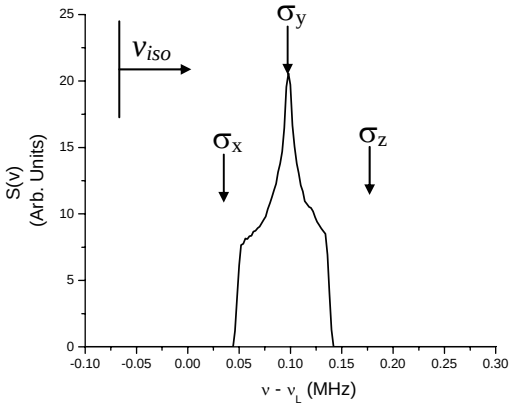

Fig. 5. NMR frequency-space powder pattern for the chemical shift. ν_L = 100 MHz, $\sigma_z = -1.4\times10^{-3}$, $\sigma_x = -5 \times 10^{-4}$, $\sigma_y = 10^{-3}$. Values of σ_i determine the positions of the shoulders and the divergence, as indicated. ν_{iso} = 96 MHz shift to higher frequencies.

In the example, we have chosen $\sigma_z = -1.4 \times 10^{-3}$, $\sigma_x = -5 \times 10^{-4}$, $\sigma_y = -10^{-3}$, which gives ν_{iso} = 96 kHz. Shifts this large have been observed for ^{125}Te (I = ½) in

crystalline Sb_2Te_3. Fig. 6 shows the measured spectra along with a simulation where $\sigma_z = \sigma_y = 0.7 \times 10^{-3}$, $\sigma_x = 1.8 \times 10^{-3}$, $\nu_L = 126.311$ MHz. Weaker, unresolved dipolar interactions are accounted for by convoluting the spectrum with a Gaussian with $\sigma_{FWHM} = 40$ kHz [3].

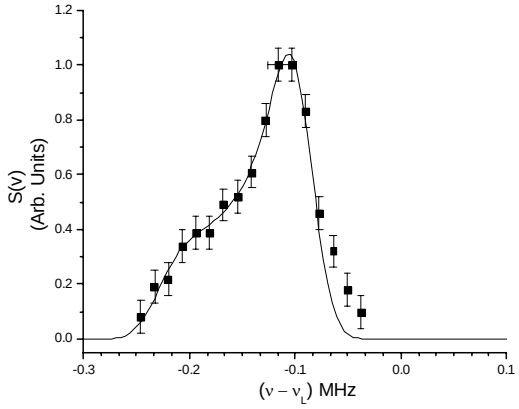

Fig. 6. Solid squares represent the experimental frequency-space NMR spectrum for ^{125}Te in crystalline Sb_2Te_3 where $\nu_L = 126.311$ MHz. The solid line is a fit based on the chemical shift interaction with $\sigma_z = \sigma_y = 0.7 \times 10^{-3}$, $\sigma_x = 1.8 \times 10^{-3}$.

In light of the recent technological interests in tellurium containing systems, i.e. Sb_2Te_3, Bi_2Te_3, and various compositions in the GeSbTe system, ^{125}Te NMR has great potential for structure measurements. ^{125}Te lacks a quadrupole moment and therefore the spectrum is simpler to interpret than for the antimony nuclei. Chemically inequivalent tellurium sites could be measured if the different shifts are adequately resolved. Future ^{125}Te NMR studies may therefore incorporate high-resolution techniques, such as magic angle spinning methods, to reduce the spectral breadth in hopes of distinguishing nonequivalent tellurium lattice sites and nearest neighbors.

c.) Combined quadrupole and magnetic shift interactions: example NMR spectra

Interpreting the data becomes increasingly difficult when more than one interaction contributes to the spectrum. When studying heavier quadrupolar nuclei, both interactions will contribute to the NMR spectrum and up to five parameters are needed to adequately explain the data. Uncoupling the contributions may be impossible if the spectrum contains no features characteristic to the interaction. To circumvent this problem it is common practice to obtain spectra under experimental conditions that accentuate certain interactions. NQR data are often coupled with NMR data to reduce the unknowns in the simulation scheme.

For adequately resolved satellite transitions (shoulders and divergences), determining the quadrupole parameters is straightforward. These features are relatively less sensitive to the chemical shift. Experimental sensitivity may limit the full line shape measurement to the more intense central region, especially in cases where ν_q is large. The problem is well demonstrated in Fig. 7, which shows the central transition at room temperature for ^{121}Sb (*I=5/2)* NMR at $\nu_L = 95.75$ MHz (400 MHz with respect to the NMR transition of hydrogen). The satellite transitions have no defining features, within experimental uncertainty, and are therefore not shown. The central transition's shape is very similar to that shown in Figs. 4b and 6, which suggests that the line shape can be adequately fit with either two quadrupole or three chemical shift parameters. A unique fit is therefore not possible using this single spectrum. Extracting the quadrupole parameters requires additional spectra. Estimates of ν_q and η based on the spectral breadth can be used as starting points for an NQR experiment. Alternatively, variations in line shape with magnetic field could provide additional constraints on the chemical shift and quadrupole parameters.

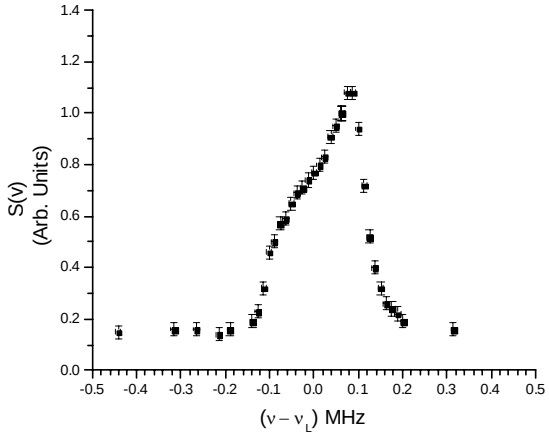

Fig. 7. Solid squares represent the experimental frequency - space NMR spectrum for ^{121}Sb in crystalline Sb_2Te_3 where $\nu_L = 95.75$ MHz.

5. Summary

The local bonding structure of disordered materials can be studied in detail using magnetic resonance methods. We have discussed general attributes of frequency spectra for both pure nuclear quadrupole and nuclear magnetic resonance in terms of parameters appearing in the total nuclear Hamiltonian. In chalcogenide glasses, the quadrupole and chemical shift interactions dominate. Frequency spectra can be fitted with calculated powder patterns for which we presented a general calculation scheme. We demonstrated some experimental challenges; such as the ambiguity in spectral fitting that arises when spectral features are unresolved. For increasingly complex systems, combining resonance data from the pure quadrupole and field dependent experiments will be critical in determining unique parameter sets.

Acknowledgements

The authors thank Professor Radu Grigorovici, to whom this paper is dedicated, for his immense contributions to the field of amorphous materials. This research was performed at the University of Utah and the Colorado School Mines under NSF grant DMR-0073004 and AFOSR grant F29601-03-01-0229.

References

[1] A. Kolobov, et al. Nature Mater. **3**, 703 (2004).
[2] D. A. Baker, Phys. Rev. Lett. **96**, 255501 (2006).
[3] P. C. Taylor, et al. Chem. Rev. **75,** 203 (1975).
[4] G. K. Semin, Physica Status Solidi A, **11**, **n 1**, K61 (1972).
[5] P. C. Taylor, J. Non-Cryst. Solids, **352**, 839 (2006).
[6] T. Su, et al. Phys. Rev. B. **67**, 085203 (2003).
[7] Z. M. Saleh, Phys. Rev. B. **40**, 10557 (1989).
[8] M. Edén, Concepts Magn. Reson. **17A**, 117 (2003).
[9] S. A. Smith, et al. J. Magn. Reson. A. **106**, 75 (1994).
[10] M. Bak, et al. J. Magn. Reson. **147**, 296 (2000).
[11] M. Veshtort, et al. J. Magn. Reson. **178**, 248 (2006).
[12] A. J. Jerschow, Magn. Reson. **176**, 7 (2005).
[13] P. Günthert, Int. J. Quantum Chem. **106**, 344-350 (2006).
[14] M. Edén, Concepts Magn. Reson. **18A**, 24-55 (2003).
[15] M. H. Cohen, Phys. Rev. **96**, 1278 (1954).
[16] W. H. Jones, et al. Phys Rev. **132**, 1898 (1963).
[17] A. Jerschow, Prog. Nucl. Magn. Reson. Spec. **46**, 63 (2005).
[18] C. P. Slichter, Principles of Magnetic Resonance (third enlarged and updated ed.), Springer Series in Solid-State Sciences, Springer Verlag (1990) January.
[19] N. F. Ramsey, Phys. Rev. **78**, 699 (1950).

*Corresponding author: craig@physics.utah.edu